

DISCOVERY OF THE LARGEST KNOWN LENSED IMAGES FORMED BY A CRITICALLY CONVERGENT LENSING CLUSTER

ADI ZITRIN & TOM BROADHURST

School of Physics and Astronomy, Tel Aviv University, Israel

Accepted to the Astrophysical Journal Letters

ABSTRACT

We identify the largest known lensed images of a single spiral galaxy, lying close to the centre of the distant cluster MACS J1149.5+2223 ($z = 0.544$). These images cover a total area of $\simeq 150 \square''$ and are magnified $\simeq 200$ times. Unusually, there is very little image distortion implying the central mass distribution is almost uniform over a wide area ($r \simeq 200 \text{ kpc}$) with a surface density equal to the critical density for lensing, corresponding to maximal lens magnification. Many fainter multiply-lensed galaxies are also uncovered by our model, outlining a very large tangential critical curve, of radius $r \simeq 170 \text{ kpc}$, posing a potential challenge for the standard Λ CDM-Cosmology. Because of the uniform central mass distribution a particularly clean measurement of the mass of the brightest cluster galaxy is possible here, for which we infer stars contribute most of the mass within a limiting radius of $\simeq 30 \text{ kpc}$, with a mass-to-light ratio of $M/L_B \simeq 4.5(M/L)_\odot$. This cluster with its uniform and central mass distribution acts analogously to a regular magnifying glass, converging light without distorting the images, resulting in the most powerful lens yet discovered for accessing the faint high- z Universe.

Subject headings: gravitational lensing , galaxies: clusters: individual: MACS J1149.5+2223 , dark matter

1. INTRODUCTION

Multiply-lensed images of distant galaxies are commonly seen near the centres of distant galaxy clusters. Thin tangentially stretched images, including giant arcs, follow an approximate ‘‘Einstein ring’’, interior to which radially directed arcs are sometimes found, pointing towards the centre of mass. The formation of such strongly lensed images requires the projected mass density to exceed a critical value, Σ_{crit} , inside the Einstein radius, given by fundamental constants and the angular-diameter distance of the lens, d_l , and of the source d_s , and their separation, d_{ls} , such that $\Sigma_{crit} = \frac{c^2}{4\pi G} \frac{D_s}{D_l D_{ls}}$. This mass density is a little less than 1 g/cm^2 for lenses at intermediate distances and comprises mainly dark matter (DM) whose nature is still unknown, with only a ~ 5 -15% contribution from gaseous baryonic material (Biviano & Salucci, 2006, Umetsu et al., 2009).

Fine examples of lensing by galaxy clusters are found at intermediate redshifts, including the most distant cluster discovered by Zwicky, Cl0024+17 ($z = 0.39$), and one of the richest clusters discovered by Abell, A1689 ($z = 0.18$), with the largest known Einstein ring, $r \simeq 45''$ (Broadhurst et al., 2005). For such clusters many tens of multiply lensed images have been identified in deep Hubble images (Broadhurst et al., 2005, Halkola et al., 2008, Limousin et al., 2008, Zitrin et al., 2009a,b), leading to accurately measured central surface mass distributions. The Einstein radii of these massive clusters are found to be larger than predicted in the context of the standard Λ CDM cosmological model (Broadhurst & Barkana, 2008, Sadeh & Rephaeli, 2008), based on the ‘‘Millenium’’ simulation (Springel et al., 2005). This discrepancy is empirically supported by the surprisingly concentrated mass profiles measured for such clusters, when combining the inner strong lensing with the outer weak lensing signal (Gavazzi et al., 2003, Broadhurst et al., 2008, Limousin et

al., 2008, Umetsu et al., 2009, Zitrin et al., 2009a, Oguri et al., 2009, Donnarumma et al., 2009) boosting the critical radius at fixed virial mass. The abundance of giant arcs may help constrain the total lensing cross section and is variously claimed to be at odds with standard Λ CDM (Bartelmann et al., 1998), though recent work favours the consensus (Dalal et al., 2004, Wambsganss et al., 2004, Horesh et al., 2005, Hennawi et al., 2007) here the selection effects are considerable and more thorough surveys should help (Hennawi et al. 2007).

The magnification generated by massive clusters has consistently led to the discovery of the highest redshift galaxies (Ebbels et al., 1995, Franx et al., 1997, Frye & Broadhurst, 1998, Bouwens et al., 2004, Kneib et al., 2004, Zheng et al., 2009), with the current record standing at $z \simeq 7.6$ for a galaxy behind A1689 (Bradley et al., 2008) and magnified by nearly a factor of ~ 10 . Although lens magnification, μ , reduces the accessible area of the source plane by $1/\mu$, it enhances the flux of faint galaxies by μ , with a net positive effect for the most distant galaxies lying on the steep exponential tail of the luminosity function (Broadhurst, Taylor & Peacock, 1995, Bradley et al., 2008). Lensing provides additional spatial resolution by stretching images, producing spatially resolved details and evidence that outflowing gas is widespread at $z > 4$ (Frye, Broadhurst & Benitez, 2002).

With the goal of discovering high redshift galaxies and to better define the mass profiles of galaxy clusters in general, we have combined data for a sample of well studied clusters. In this process we have uncovered the unusual lensing properties of MACS J1149.5+2223 ($z=0.544$), a cluster originally identified in the highly complete sample of the most X-ray luminous clusters in the Universe (Ebeling et al., 2007). In §2 we describe the observations, in §3 we describe the lensing analysis and results, in §4 we address the BCG, and in §5 discuss our conclusions. Throughout the paper we adopt the standard cosmology

($\Omega_{m0} = 0.3$, $\Omega_{\Lambda0} = 0.7$, $h = 0.7$). Accordingly, one arc-second corresponds to 6.4 kpc/ h_{70} at the redshift of this cluster. The reference center of our analysis is fixed at the center of the cD galaxy: RA = 11:49:35.70, Dec = +22:23:54.8 (J2000.0).

2. OBSERVATIONS

The central region of the luminous X-ray cluster MACS J1149.5+2223 ($z = 0.544$) has been imaged in April 2004 and in May 2006, with the Wide Field Channel (WFC) of the ACS installed on HST. Integration times of $\sim 4500s$ were obtained through the F555W and the F814W filters. We retrieved these images (PI: Ebeling, proposal ID: 9722) found in the Hubble Legacy Archive. Several large blue spiral galaxy images are clearly visible near the central brightest cluster galaxy (Figures 1-3). On closer inspection, individual HII regions and spiral arms are repeated very clearly in images 1.1 and 1.2, demonstrating beyond question that these are images of the same source, even though they do not appear as thin distorted arcs. The other central spiral galaxy images seen in Figure 1-3 are also images of the same source but with differing mirror symmetry (parity), as we show below. Image 1.2 is the largest, covering an area of $\simeq 55 \square''$, and in total $\gtrsim 150 \square''$ is subtended by all the images of this source, several times greater than the largest giant arc known (Soucail et al., 1987).

Many other faint lensed galaxies are also visible, generally at larger distances from the centre (marked in Figure 2) indicating that they lie at higher redshift and most of which we have been able to securely identify as sets of multiply-lensed background galaxies as detailed below.

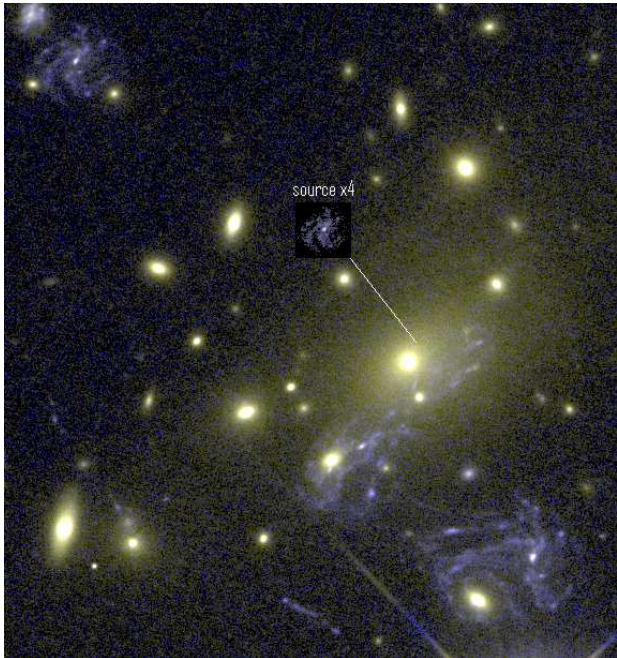


FIG. 1.— The central region of the cluster MACS J1149.5+2223 ($z = 0.544$) imaged with Hubble/ACS in V and I-bands, showing the several large, well resolved, blue spiral galaxy images centered on the brightest red cluster member galaxy (cD). The small de-lensed source, zoomed-in $\times 4$ to show internal details, is inset near its predicted location demonstrating the very large magnifications generated by the central gravitational field of this cluster.

3. LENSING ANALYSIS

We apply our well tested approach to lens modelling, which we have applied successfully to A1689 and Cl0024, uncovering unprecedentedly large numbers of multiply-lensed images (Broadhurst et al., 2005, Zitrin et al., 2009a). The full details of this approach can be found in these papers. Briefly, the basic assumption adopted is that mass approximately traces light, so that the photometry of the red cluster member galaxies is the starting point for our model.

Cluster member galaxies are identified as lying close to the cluster sequence by the photometry provided in the Hubble Legacy Archive. We approximate the large scale distribution of matter by assigning a power-law mass profile to each galaxy, the sum of which is then smoothed. The degree of smoothing and the index of the power-law are the most important free parameters. A worthwhile improvement in fitting the location of the lensed images is generally found by expanding to first order the gravitational potential of the smooth component, equivalent to a coherent shear, where the direction of the shear and its amplitude are free, allowing for some flexibility in the relation between the distribution of DM and the distribution of galaxies which cannot be expected to trace each other in detail. The total deflection field $\vec{\alpha}_T(\vec{\theta})$, consists of the galaxy component, $\vec{\alpha}_{gal}(\vec{\theta})$, scaled by a factor K_{gal} , the cluster DM component $\vec{\alpha}_{DM}(\vec{\theta})$, scaled by $(1-K_{gal})$, and the external shear component $\vec{\alpha}_{ex}(\vec{\theta})$:

$$\vec{\alpha}_T(\vec{\theta}) = K_{gal}\vec{\alpha}_{gal}(\vec{\theta}) + (1 - K_{gal})\vec{\alpha}_{DM}(\vec{\theta}) + \vec{\alpha}_{ex}(\vec{\theta}), \quad (1)$$

where the deflection field at position $\vec{\theta}_m$ due to the external shear, $\vec{\alpha}_{ex}(\vec{\theta}_m) = (\alpha_{ex,x}, \alpha_{ex,y})$, is given by:

$$\alpha_{ex,x}(\vec{\theta}_m) = |\gamma| \cos(2\phi_\gamma) \Delta x_m + |\gamma| \sin(2\phi_\gamma) \Delta y_m, \quad (2)$$

$$\alpha_{ex,y}(\vec{\theta}_m) = |\gamma| \sin(2\phi_\gamma) \Delta x_m - |\gamma| \cos(2\phi_\gamma) \Delta y_m, \quad (3)$$

where $(\Delta x_m, \Delta y_m)$ is the displacement vector of the position $\vec{\theta}_m$ with respect to a fiducial reference position, which we take as the lower-left pixel position (1, 1), and ϕ_γ is the position angle of the spin-2 external gravitational shear measured anti-clockwise from the x -axis. The normalisation of the model and the relative scaling of the smooth DM component versus the galaxy contribution brings the total number of free parameters in the model to 6.

We lens all well detected candidate lensed galaxies back to the source plane using the derived deflection field, and then relens this source plane to predict the detailed appearance and location of additional counter images, which may then be identified in the data by morphology, internal structure and colour. The fit is assessed by the RMS uncertainty in the image plane:

$$RMS_{images}^2 = \sum_i ((x'_i - x_i)^2 + (y'_i - y_i)^2) / N_{images}, \quad (4)$$

where x'_i and y'_i are the locations given by the model, and x_i and y_i are the real images location, and the sum is over all N_{images} images. The best-fit solution is unique in this context, and the uncertainties are determined by the location of predicted images in the image plane.

Importantly, this image-plane minimisation does not suffer from the well known bias involved with source plane

minimization, where solutions are biased by minimal scatter towards shallow mass profiles with correspondingly higher magnification. The model is successively refined as additional sets of multiple images are identified and then incorporated to improve the model (Zitrin et al., 2009a).

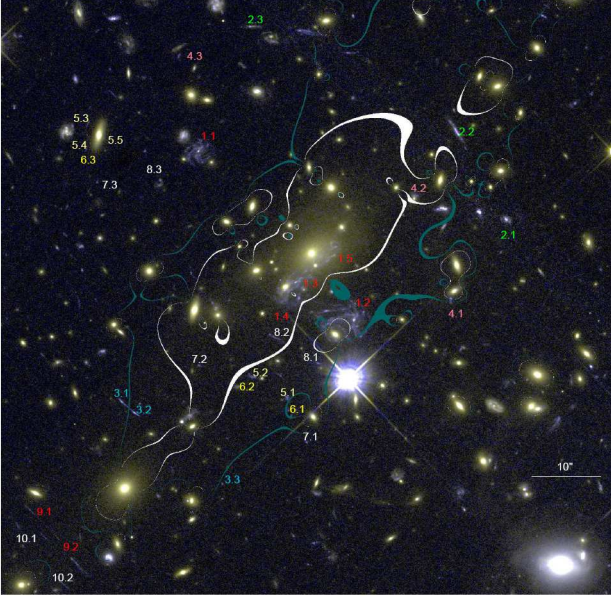


FIG. 2.— Large scale view of the multiply lensed galaxies identified by our model. In addition to the large spiral galaxy system 1, many other fainter sets of multiply lensed galaxies are uncovered by our model. The white curve overlaid shows the tangential critical curve corresponding to the distance of system 1. The larger critical curve overlaid in blue corresponds to the average distance of the fainter systems, passing through close pairs of lensed images in systems 2 and 3. This large scale elongated “Einstein ring” encloses a very large critically lensed region equivalent to 170 kpc in radius. For this cluster one arcsecond corresponds to 6.4 kpc/h_{70} , with the standard cosmology.

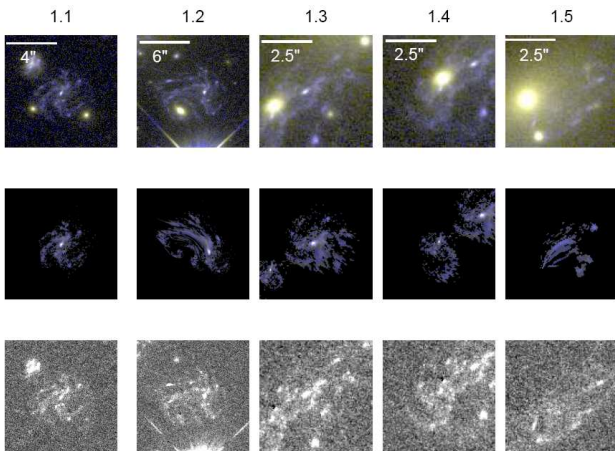


FIG. 3.— The observed images are shown with (top row) and without (bottom row) the light of the cluster member galaxies, and compared with our model generated images (middle row). For the model we take as input the pixels belonging to 1.1, the least distorted and cleanest image in system 1, and delens these pixels back to the source plane (see inset in figure 1) and then relens the source plane to generate counter images. It is clear that our modelling is successful in demonstrating the multiply-lensed origin of all 5 observed images, corresponding to a single distant spiral galaxy.

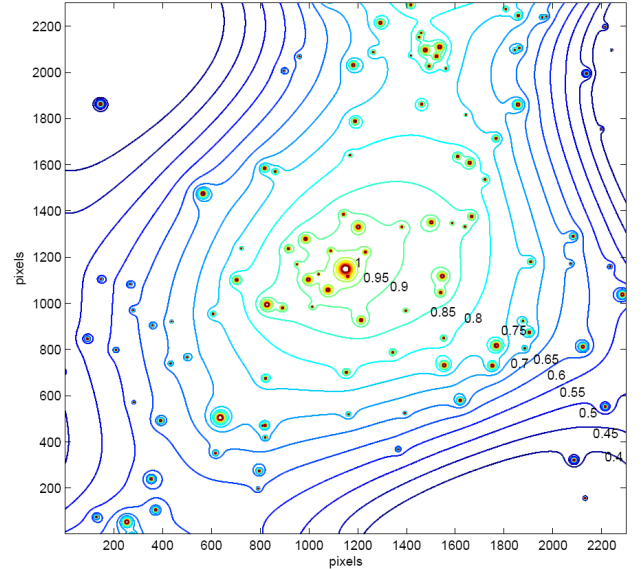


FIG. 4.— 2D surface mass distribution (κ), in units of the critical density. Contours are shown in linear units, derived from the mass model constrained using 33 multiply lensed images seen in Figure 2. Note, the central mass distribution is shallow, and rounder in shape than the critical curves.

The derived surface mass distribution is found to be very nearly uniform within the central $\simeq 200$ kpc (Figures 4-5), with very little uncertainty, as must be expected given the very large and undistorted images observed. The value of the uniform surface mass in this central region is the critical value for generating multiple images, about $\simeq 0.50$ g/cm^2 at our estimated redshift for the source, see below.

The total magnification of the spiral galaxy we derive is about, $\simeq 200$, when summed over all five images, forming the largest known images of any lensed source, and is independent of the unknown source redshift, and given by the ratio of the area of images divided by the area subtended by the deprojected source. This can be appreciated in Figure 1 where we plot for comparison the unlensed source and its modelled location on the sky, whose diameter is estimated to be $\simeq 0.9''$, typical of unlensed spiral galaxies at intermediate redshifts.

The critical curve corresponding to the spiral system is shown in Figure 2, together with the larger Einstein radius derived for the fainter galaxies, which lie at higher redshift, typically in the range $z \sim 1.5 - 2.5$, based on other massive clusters where redshift measurements have been made or photometric redshifts obtained with more colour information (Broadhurst et al., 2005, Zitrin et al., 2009a). From this we can roughly calculate the relative lensing distance of the spiral system 1, from the ratio d_{ls}/d_s . For a mean background redshift of $z = 1.5$, the spiral system is at $z \simeq 1.2$, and at the other extreme for a background redshift of $z = 2.5$ the maximum predicted redshift of the spiral is $z \simeq 2$. Assuming an average background depth of $z \simeq 2 \pm 0.5$ yields $z_{spiral} = 1.5^{+0.5}_{-0.3}$, due to the shape of the d_{ls}/d_s growth as a function of source redshift for a cluster at $z = 0.544$. The shape, location and magnification of the critical curves are unaffected by this uncertainty.

The tangential critical curve is elongated, with a major axis of $\sim 80''$ at a redshift of ~ 2 (Figure 2), reflecting the somewhat elongated distribution of matter (Figure 4). Note, the mass distribution is more symmetric than the shape of the tangential critical curve, the form of which is sensitive to asymmetry. The circular equivalent Einstein radius contained within the critical area is $\simeq 27''$ for faint sources at $z \sim 2$, corresponding to the outer tangential critical curve drawn in Figure 2 (light blue curve), which in physical units is $170 \pm 20 \text{ kpc}$ at the distance of the cluster, where the uncertainty is dominated by the uncertain mean redshift of the background galaxies. Note that because of the weak redshift dependence of lensing distance, d_{ls}/d_s , the uncertain redshifts are only a minor source of uncertainty when deriving physical scales.

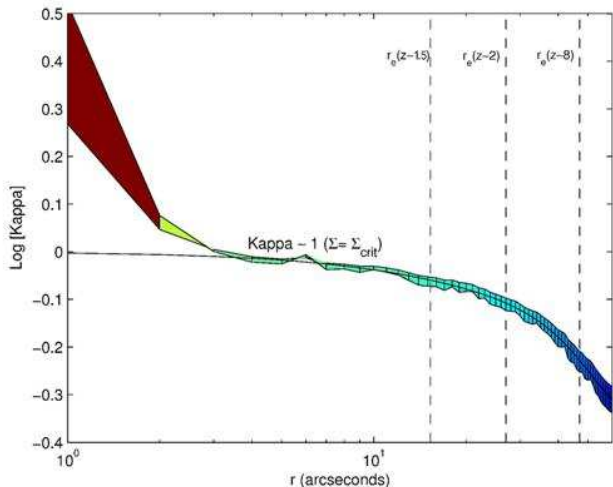


FIG. 5.— Radial surface mass density profile, $\kappa(r)$, in units of the critical surface density, i.e. $\kappa(r) = \Sigma(r)/\Sigma_{crit}$, derived for the range of radius covered by all sets of multiple images shown in Figure 2. The profile is very flat within $\sim 200 \text{ kpc}$, at a level equal to the critical density for system 1 (black line). The rise in the centre below $\sim 5''$ is due to the contribution of the cD galaxy, under which the modelled smooth cluster mass component is indicated by the black line. Three geometrically averaged Einstein radii are indicated, corresponding to $16''$ radius for system 1, and $27''$ at the mean depth of the fainter systems ($z \simeq 2$) and $47''$ is predicted for the Einstein radius at high redshift, $z \simeq 8$.

4. BRIGHTEST CLUSTER GALAXY

The mass profiles of brightest cluster galaxies are not very well constrained presently by lensing, but may help elucidate the origin of these poorly understood class of objects (von der Linden et al., 2007, and references therein). The best studied example with lensing is MS2137 (Gavazzi et al., 2003, Donnarumma et al., 2009), where radial arcs lie close to this object. For clusters like A1689 and Cl0024+17 there are too many massive galaxies in the central region to allow a unique determination of the brightest galaxy. Here we are fortunate to have such extended lensed images spread over a wide range of radius to help constrain the central mass distribution. Furthermore, the contrast of the cD mass above the flat cluster profile is clear, allowing an accurate subtraction of the cluster contribution, as shown in Figure 5. We model this galaxy analytically as a general power-law mass profile with a projected core (Barkana 1998), resulting in a mass of $\sim 1.0 \pm 0.2 \times 10^{12} M_{\odot}$ interior to the limiting radius of $\simeq 30 \text{ kpc}$ traced by the

low surface brightness wings of the light profile (see Figure 1), where the uncertainty is dominated by the gradient of the cD mass profile (Figure 5).

Integrating the light within this radius yields $2.2 \times 10^{11} L_{\odot}$, in the restframe B-band and hence a mean mass-to-light ratio of $\sim M/L_B = 4.5 \pm 1 (M/L)_{\odot}$. This ratio can be fully accounted for by the stars contained in this galaxy, for which we obtain $M/L_B \simeq 5 (M/L)_{\odot}$, for a single burst stellar population formed at $z = 3$ and viewed at a redshift of $z = 0.544$, equivalent to an age of $\sim 6 \text{ Gyr}$ s, and with a mean metallicity of half solar. Other lensing work supports relatively low mass-to-light for the cD galaxy in MS2137 ($M/L < 10 (M/L)_{\odot}$, Gavazzi et al., 2003), with less direct estimates relying on dynamical motions showing evidence for non-stellar DM at larger radius for other cD galaxies (Dressler 1979, Gebhardt & Thomas, 2009). This demonstrates the need for more thorough studies of these enigmatic objects.

5. DISCUSSION

The unusually large and undistorted lensed images of a spiral galaxy uncovered here requires a nearly uniform distribution of matter within the central $\sim 200 \text{ kpc}$ region covered by these images. The formation of multiple images requires the value of the central surface density to be nearly equal to the critical surface density for lensing. This lens corresponds to the case of maximum magnification, given by the general relation $\mu = (((1 - (\Sigma/\Sigma_{crit})^2 - \gamma^2))^{-1}$, because the lensing shear, γ , vanishes for a uniform density and therefore the magnification diverges when the surface density is equal to the critical density, $\Sigma = \Sigma_{crit}$. These conclusions follow from the fundamentals of lensing and do not rely on any model.

In detail we show that the locations and parity of the lensed images can be accurately reproduced with a simple model where indeed the central mass distribution is nearly uniform and the magnification derived is very large, $\times 200$, independent of the source redshift. This model is used to identify 9 additional sets of fainter multiply lensed images, which are incorporated to improve the fit, so that the final model comprising 6 free parameters, is constrained by a total of 33 lensed images. These fainter images are deflected by larger angles than the bright lensed spiral galaxy placing their images generally further from the cluster center.

From our model, the circular equivalent Einstein radius contained within the critical area is $\simeq 27''$ for faint sources at $z \sim 2$, corresponding to the outer tangential critical curve (drawn in Figure 2), which in physical units is $170 \pm 20 \text{ kpc}$ at the distance of the cluster. This very large radius adds to the already uncomfortable discrepancy between the large Einstein radii observed for massive clusters and the predictions based on the standard LCDM cosmology (Broadhurst & Barkana, 2008, Sadeh & Rephaeli, 2008, Puchwein & Hilbert, 2009) for which such large Einstein radii can only be contemplated with mass distributions which are prolate and aligned along the line of sight (Corless & King, 2007, Oguri & Blandford, 2009). Instead, here the cluster is evidently elongated across the line of sight, traced by the bright galaxies, extended X-ray emission (see Figure 1 in Ebeling et al., 2007) and the critical curves (see Figure 2). The central mass distribution is evidently unconcentrated, and presumably related to its

currently unrelaxed state.

The velocity field of the lensed spiral can be readily obtained because of the large solid angle covered by each lensed image, and if the inclination can be reliably derived from such data then an independent estimation of the magnification can be derived via the Tully-fisher relation. Spectroscopy of the internal velocity dispersion of the starlight of the cD galaxy will also help in understanding the cD mass profile, for which we have shown, rather surprisingly, seems to be dominated by stars out to the observable limit of 30 kpc.

This cluster is unique in having near uniform density in projection, at the critical level, thereby maximising gravitational lens magnification. We calculate that the total area of sky exceeding a magnification, $\mu > 10$, is ~ 2.8 square arcminutes, corresponding to the current high redshift limit of $z \sim 8$, which is over twice the equivalent area calculated for other massive clusters such as A1689

(Broadhurst et al., 2005) and Cl0024 (Zitrin et al., 2009a). This extreme magnification together with the lack of image distortion makes MACS J1149.5+2223 the most powerful known lens for accessing faint galaxies in the early universe.

ACKNOWLEDGMENTS

We are grateful for the hospitality of ASIAA, where part of this work was accomplished. We thank our anonymous referee for useful comments, and acknowledge useful discussions with Craig Sarazin, Holland Ford and Wei Zheng. ACS was developed under NASA contract NAS 5-32865. This research is based on observations provided in the Hubble Legacy Archive which is a collaboration between the Space Telescope Science Institute (STScI/NASA), the Space Telescope European Coordinating Facility (ST-ECF/ESA) and the Canadian Astronomy Data Centre (CADM/NRC/CSA).

REFERENCES

- Barkana, R., 1998, *ApJ*, 502, 531
 Bartelmann, M., Huss, A., Colberg, J.M., Jenkins, A., Pearce, F.R., 1998, *A&A*, 330, 1
 Biviano, A., Salucci, P., 2006, *A&A*, 452, 75
 Bouwens, R.J., et al., 2004, *ApJ*, 616, 79
 Bradley, L.D., et al., 2008, *ApJ*, 678, 647
 Broadhurst, T.J., Taylor, A.N., Peacock, J.A., 1995, *ApJ*, 438, 49
 Broadhurst, T., et al., 2005, *ApJ*, 621, 53
 Broadhurst, T.J. & Barkana R., 2008, *MNRAS*, 390, 1647
 Broadhurst, T., Umetsu, K., Medezinski, E., Oguri, M., Rephaeli, Y., 2008, *ApJ* 685, L9
 Corless, V.L., King, L.J., 2007, *MNRAS*, 380, 149
 Dalal, N., Holder, G., Hennawi, J.F., 2004, *ApJ*, 609, 50
 Donnarumma, A., Etori, S., Meneghetti, M., Moscardini, L., 2009, arXiv0902.4051
 Dressler, A., 1979, *ApJ*, 231, 659
 Ebbels, T.M.D., Le Borgne, J.-F., Pello, R., Ellis, R.S., Kneib, J.-P., Smail, I., Sanahuja, B., 1996, *MNRAS*, 281, 75
 Ebeling, H., et al., 2007, *ApJ*, 661, 33
 Franx, M., Illingworth, G.D., Kelson, D.D., van Dokkum, P.G. & Tran, K., 1997, *ApJ*, 486, 75
 Frye, B. & Broadhurst, T., 1998, *ApJ*, 499, 115
 Frye, B., Broadhurst, T., Benítez, N., 2002, *ApJ*, 568, 558
 Gavazzi, R., Fort, B., Mellier, Y., Pello, R., Dantel-Fort, M., 2003, *A&A*, 403, 11
 Gebhardt, K., Thomas, J., 2009, arXiv0906.1492
 Halkola, A., et al., 2008, *A&A*, 481, 65
 Hennawi, J.F., Dalal, N., Bode, P., Ostriker, J.P., 2007, *ApJ*, 654, 714
 Horesh, A., Ofek, E.O., Maoz, D., Bartelmann, M., Meneghetti, M., Rix, H.-W., 2005, *ApJ*, 633, 768
 Kneib, J.-P., Ellis, R.S., Santos, M.R., Richard, J., 2004, *ApJ*, 607, 697
 Limousin, M., et al., 2008, *A&A*, 489, 23
 Oguri, M., et al., 2009, arXiv0901.4372
 Oguri, M., Blandford, R.D., 2009, *MNRAS*, 392, 930
 Puchwein, E. & Hilbert, S., 2009, arXiv0904.0253
 Sadeh, S. & Rephaeli, Y., 2008, *MNRAS*, 388, 1759
 Soucail, G., Fort, B., Mellier, Y., Picat, J. P., 1987, *A&A*, 172, 14
 Springel, V., et al., 2005, *Nature*, 435, 629
 Umetsu, K., et al., 2009, *ApJ* 694, 1643
 von der Linden, A., Best, P.N., Kauffmann, G., White, S.D.M., 2007, *MNRAS*, 379, 867
 Wambsganss, J., Bode, P., Ostriker, J.P., 2004, *ApJ*, 606L, 93
 Zheng, W., et al., 2009, *ApJ*, 697, 1907
 Zitrin, A., et al., 2009a, *MNRAS*, 396, 1985
 Zitrin, A., Broadhurst, T., Rephaeli, Y., Sadeh, S., 2009b, arXiv0907.4232